



HAL
open science

Cleaved CD95L perturbs in vitro macrophages responses to *Toxoplasma gondii*

Ellen A Tiffney, Janine L Coombes, Patrick Legembre, Robin J Flynn

► To cite this version:

Ellen A Tiffney, Janine L Coombes, Patrick Legembre, Robin J Flynn. Cleaved CD95L perturbs in vitro macrophages responses to *Toxoplasma gondii*. *Microbes and Infection*, 2022, 24 (5), pp.104952. 10.1016/j.micinf.2022.104952 . hal-03632273

HAL Id: hal-03632273

<https://hal.science/hal-03632273>

Submitted on 12 Apr 2022

HAL is a multi-disciplinary open access archive for the deposit and dissemination of scientific research documents, whether they are published or not. The documents may come from teaching and research institutions in France or abroad, or from public or private research centers.

L'archive ouverte pluridisciplinaire **HAL**, est destinée au dépôt et à la diffusion de documents scientifiques de niveau recherche, publiés ou non, émanant des établissements d'enseignement et de recherche français ou étrangers, des laboratoires publics ou privés.



Distributed under a Creative Commons Attribution - NonCommercial 4.0 International License

1 **Short communication**

2 **Title:** Cleaved CD95L perturbs *in vitro* macrophages responses to *Toxoplasma gondii*

3 **Authors:** Ellen A. Tiffney¹, Janine L. Coombes¹, Patrick Legembre², Robin J Flynn^{1,3*}

4 **Addresses:**

5 ¹ Dept. Infection Biology, Institute of Infection and Global Health, University of Liverpool, L3

6 5RF,

7 ² Centre Eugène Marquis, Université Rennes-1, INSERM U1242, Rennes, France.

8 ³ Graduate Studies Office, Department of Research, Innovation and Graduate Studies,

9 Waterford Institute of Technology, Ireland, X91 K0EK.

10 **Correspondence** *Robin J Flynn, Graduate Studies Office, Department of Research,
11 Innovation and Graduate Studies, Waterford Institute of Technology, Cork Road, Ireland, X91
12 K0EK. robin.flynn@wit.ie, Tel +353 (0) 85 862 2662, Fax +353 (0) 51 30 2000.

13

14

15 **Abstract**

16 *Toxoplasma gondii* infects approximately 1-2 billion people, and manipulation of the
17 macrophage response is critical to host and parasite survival. A cleaved (cl)-CD95L form can
18 promote cellular migration and we have previously shown that cl-CD95L aggravates
19 inflammation and pathology in systemic lupus erythematosus (SLE). Findings have shown
20 that CD95L is upregulated during human infection, therefore we examined the effect of cl-
21 CD95L on the macrophage response to *T. gondii*. . We find that cl-CD95L promotes parasite
22 replication in macrophages, associated with increased arginase-1 levels, mediated by signal
23 transducer and activator of transcription (STAT)6. Inhibition of both arginase-1 and STAT6
24 reversed the effects of cl-CD95L. Phospho-kinase array showed that cl-CD95L alters Janus
25 Kinases (JAK)/STAT, mammalian target of rapamycin (mTOR), and Src kinase signals. By
26 triggering changes in JAK/STAT cl-CD95L may limit anti-parasite effectors.

27 **Keywords:** *Toxoplasma gondii*; macrophage; CD95L; FasL; JAK/STAT; arginase; cleaved CD95L

28

29

30 1. Introduction.

31 *Toxoplasma gondii* is an obligate intracellular parasite capable of causing significant disease
32 in both human and animal hosts. *T. gondii* has the ability to infect multiple cell types but
33 preferentially infects monocytes or dendritic cells (DCs). Within these cells *T. gondii* is
34 effectively able to control the host cell niche. Studies have demonstrated that parasite
35 secreted effectors alter macrophage functions and their regulating signalling mechanisms
36 [1]. Indeed, multiple effectors target the JAK-STAT cascade and confer virulence in
37 recombinant avirulent strains of parasite [2]. This is a two-sided process, host priming of the
38 macrophage is key to effective parasite control and incorrect priming, resulting in arginase-1
39 producing macrophage, cannot restrain parasite replication [3].

40 The CD95-CD95L (also known as Fas-FasL, respectively) interaction is key to controlling
41 intracellular parasites via induction of cellular apoptosis [4]. Indeed, appropriate CD95
42 signalling post-infection is thought to control immunopathology [5]. Studies [6] have shown
43 that *T. gondii* can inhibit CD95 mediated killing by impairing the correct functioning of
44 caspase 8. Recently, CD95L has been shown to undergo a metalloprotease-mediated
45 cleavage event leading to a soluble, cl-CD95L that drives cellular migration rather than
46 death [4]. Additionally, we have recently shown that cl-CD95L causes exacerbated pathology
47 during the onset of murine lupus due to increased cellular infiltration within inflamed tissues
48 [7]. A previous survey of pregnant human toxoplasmosis patients had shown that this form
49 of CD95L increased during chronic infection [8] and *in vitro* infection with *T. gondii* RH
50 induced high levels of soluble cl-CD95L in both macrophages and trophoblast cells [9].

51 Given these findings we sought to directly assess the effect of soluble cl-CD95L on the
52 outcome of macrophage infection with *T. gondii*. We report that cl-CD95L leads to increased

53 parasite replication partially dependent on changes in IL-6 and arginase-1 levels.
54 Interestingly, these opposing mechanisms may be explained by the finding that cl-CD95L
55 reprograms macrophages to acquire a Myeloid-Derived Suppressor Cell (MDSC)-like
56 phenotype.

57

Journal Pre-proof

58 2. Methods

59 2.1 Parasite Culture.

60 Host VERO cells were cultured in DMEM supplemented with 5% fetal bovine serum (FBS,
61 F4135 Sigma Aldrich), penicillin-streptomycin (10,000 U penicillin & 100 mg/ml streptomycin
62 (Sigma Aldrich) at 5% CO₂ at 37°C in 25 cm² flasks until cells were 80% confluent. The RH
63 strain of *T. gondii* was used throughout the work. Parasites were propagated as tachyzoites
64 by serial passage in VERO cells. For the purification of *T. gondii* tachyzoites, infected host
65 VERO cells were dislodged from culture flasks by scrapping with a single-use rubber cell
66 scraper. Dislodged cells were passed, through a sterile blunt-ended needle. Lysed cells and
67 isolated parasites were centrifuged at 2,000 rpm for 10 minutes at room temperature (RT).
68 Parasites were resuspended in 5 mL 1X D-PBS and this solution was added to a PD-10
69 column, columns were then washed with 5 mL 1X D-PBS. The number of parasites recovered
70 was counted in 10 µL of parasite solution. Finally, the parasites were centrifuged for 10
71 minutes at 2,000 rpm, supernatant removed and resuspended in complete DMEM.

72 2.2 Bone marrow-derived macrophages (BMDM).

73 Bone marrow-derived macrophages were obtained from healthy wild-type C57Bl/6 mice
74 aged between 8-16 weeks. Animals were culled by standard schedule 1 procedures of
75 exposure to rising concentrations of CO₂. Immediately afterwards hind femurs were
76 removed and placed into sterile D-PBS for transport to the laboratory. Excess fat, muscle,
77 and skin were removed. Thereafter, the bone marrow was flushed from the femur by
78 repeated injecting, using a 2 mL syringe and a 25-gauge needle, of the femur with complete
79 media. Cells were passed through a 70 µm cell strainer and centrifuged for 10 minutes at

80 1,500 rpm. Bone marrow cells were seeded at 2×10^6 /mL in a 6 mL petri dish with the
81 addition of 20 ng/mL of M-CSF (Recombinant Murine M-CSF, PeproTech). Every two days the
82 media and M-CSF was replenished until cells were harvested on day 7. Thereafter
83 macrophages were seeded in 96 well flat-bottomed plates (Greiner Bio-One) at 2×10^4 /well.
84 In some experiments chemical inhibitors or antibodies were added to cultures prior to
85 infection as follows; anti-mouse IL-6 (BioXCell Clone MP5-20F3) was used at 120 ng/mL; to
86 inhibit Arginase, N^{ω} -hydroxy-nor-Arginine (nor-NOHA) (Sigma) was used at 5 mM; to inhibit
87 cl-CD95L, mFas-Fc Chimera (R&D Systems Cat No. 435-FA) was added at 200 ng/mL; and to
88 inhibit STAT6, the compound AS1517499 (Sigma) was used at 0.2 mg/mL.

89

90 *2.3 Percentage monolayer destruction and free parasite counts*

91 VERO cells or BMDM were seeded into 24 well plates at 2.5×10^4 /well and incubated for 24
92 hours. Thereafter, cells were stimulated with cl-CD95L at indicated doses and 24 hours later
93 cells were infected with *T. gondii* at 1×10^5 /well (MOI 4). After 3 hours the medium was
94 changed to remove free extracellular parasites and replaced with fresh media. Thereafter,
95 cells were incubated for 72 hours. After 72 hours post-infection the percentage of the VERO
96 monolayer that has been destroyed was estimated using an Olympus BH2 microscope at X10
97 magnification, using a previously described method [10]. In brief, a counting grid was
98 overlaid onto images and consistent squares were counted across images. Destruction was
99 recorded were 50% of cells within a grid square no longer had an intact membrane. An
100 aliquot of supernatant was used to determine the extracellular parasite load.

101 *2.4 ATP and Cytokine Detection*

102 Supernatants were collected from BMDM cultures and used for CellTiter-Glo assays for the
103 detection of ATP. 100 μ L of each sample and media controls, as background controls, were
104 added to a 96-well opaque plate. The plate was then left at RT for 30 minutes to equilibrate.
105 Thereafter, 100 μ L of CellTiter-Glo[®] Reagent was added to each well. The contents were then
106 mixed for 2 minutes on an orbital shaker, followed by a 10 minutes incubation at RT.
107 Luminescence was then recorded using a luminometer. Cytokine ELISAs for IL-6 and IL-1 β
108 were conducted using commercially available kits from Invitrogen (Cat no. 88-7064-88, 88-
109 7013, respectively).

110 *2.5 Arginase assay.*

111 Cell lysates were prepared in Triton X-100. 50 μ L of 10 mM MnCl₂/50 mM Tris-HCl buffer (pH
112 7.5) and 50 μ L of lysate were mixed and incubated for 10 minutes at 55°C for enzyme
113 activation. 50 μ L of 0.5 M L-arginine substrate (pH 9.7) was added to the activated lysate
114 and incubated for 1 hour at 37°C. To stop the reaction the acid-stop solution that was
115 comprised of H₂SO₄ (96%), H₃PO₄ (85%), and H₂O in a ratio of 1:3:7 was added to the
116 samples. Finally, 9% isonitrosopriophenone was added to develop colour. The sample was
117 then heated to 103°C for 45 minutes and allowed to cool in darkness for another 10 minutes.
118 200 μ L aliquots are then added to a 96 well ELISA plate and absorbance measured at 540
119 nm.

120 *2.6 BMDM Phospho-Kinase Array*

121 To determine a global signalling profile a Phospho-Kinase Array Proteome Profiler was used
122 (R&D Systems, Cat No. ARY003B) BMDM were either left unstimulated or stimulated with
123 100 ng/mL of cl-CD95L for 24 hours, after which macrophages were rinsed with D-PBS.

124 Macrophages were then solubilised at 1×10^7 cells/mL in Lysis Buffer 6 (R&D systems).
125 Samples were pipetted up and down in order to resuspend macrophages and incubated for
126 30 minutes at 2-8°C. Samples were then microcentrifuged and the supernatant transferred
127 to an Eppendorf tube. Membranes were placed in the wells of an 8-Well Multi-dish and filled
128 with 1.0 mL of Assay Buffer 1, which served as a blocking buffer. The plate was incubated on
129 a rocking platform shaker for 1 hour. Membranes were then washed in 20 mL of wash
130 buffer. After which, 1.0 mL of prepared samples were added to both parts A and B of each
131 membrane. The plate was then incubated on a rocking platform shaker overnight at 2-8°C.
132 Then 1.0 mL of reconstituted Detection Antibody Cocktail in Assay Buffer was added to each
133 well and incubated with shaking for 1 hour at RT. After, 1.0 mL of diluted Steptavidin-HRP in
134 Array Buffer 2/3 was added to each well of the plate and incubated with shaking for 30
135 minutes at RT. Membranes were then washed. After washing, 1.0 mL of Chemi-Reagent Mix
136 was added to each membrane and incubated for 1 minute. After incubation, excess Chemi-
137 Reagent Mix was removed from each membrane. Membranes were imaged using a
138 ChemiDoc. Pixel Density was measured using ImageJ software. The pixel density was
139 normalised to total protein concentration in each lysate as determined by BCA assay.

140

141 *2.7 Statistics*

142 Raw data was collected on Microsoft Excel workbooks. All data analysis was conducted using
143 Prism 7 (GraphPad). P values of < 0.05 were taken as significant, the details of individual
144 tests are reported in the figure legends.

145

146 3. Results

147 3.1 Cleaved-CD95L alters *T. gondii* replication within host cells.

148 We initially tested the effect of pre-treatment of the VERO cell line with cl-CD95L prior to
149 infection with *T. gondii*. Infection with *T. gondii* alone increases cellular destruction from 2%
150 in uninfected/unstimulated to 14% in infected/unstimulated (Fig.1A; $P < 0.01$). VERO cells
151 were stimulated with 100 ng/mL of cl-CD95L and then infected with *T. gondii*, giving rise to
152 26% cellular destruction that is statistically significant compared with stimulated but
153 uninfected cells (Fig. 1A; $P < 0.01$). The difference in cellular destruction between infected
154 cultures when cl-CD95L was present was also statistically significantly different, $P < 0.01$ (Fig.
155 1A). Host cell destruction is often an indicator of cell egress. The number of parasites in the
156 supernatant was determined after 48 hours of infection by manual counting. Figure 1B
157 demonstrates that a significant increase in parasite replication occurs after stimulation with
158 cl-CD95L (12×10^4 /mL parasites) when compared to unstimulated VERO cells (9×10^4 /mL
159 parasites; P value < 0.05). Having demonstrated that the increase in monolayer destruction
160 above might be caused by the increase in *T. gondii* load following cl-CD95L stimulation we
161 sought to determine if cl-CD95L was causing these effects by decreasing cell viability. We
162 assessed extracellular ATP in supernatants, the results show that before infection, as
163 expected, there are high levels of cell viability as indicated by high levels of ATP (Fig.1C). In
164 comparison, after infection with *T. gondii* the levels of cell viability, in both unstimulated and
165 stimulated conditions decrease (P value < 0.001).

166 To ensure our results were representative of primary host cells, we assessed the effect of cl-
167 CD95L in murine macrophages. Bone marrow derived macrophages (BMDMs) were matured
168 from bone marrow in the presence of M-CSF for 7 days prior to collection and further use.

169 We investigated the impact of stimulation with cl-CD95L on parasite replication in BMDM by
170 performing parasite counts after 48 hours of infection. As shown Figure 1D, a significant
171 increase in parasite counts occur after BMDM cultures have been stimulated with cl-CD95L
172 when compared to unstimulated cultures (P value <0.05). Additionally, we demonstrated
173 that the effects observed were directly due to cl-CD95L by use of a Fas-Fc fusion protein to
174 compete with cl-CD95L [7]. Figure 1E demonstrates that in the presence of the decoy
175 receptor CD95-Fc, parasite replication levels were not significantly different from untreated
176 infected controls.

177

178 3.2 cl-CD95L alters arginase-1 and IL-6 levels during *T. gondii* infection.

179 To determine if the increase in parasite load, mediated by cl-CD95L, paralleled changes in
180 the BMDM response to infection we measured IL-6 in the supernatants of infected BMDMs
181 in presence or absence of cl-CD95L. Figure 2A clearly demonstrates that cl-CD95L treatment
182 alone did not drive the increase in IL-6 alone but did elicit an increase in IL-6 in combination
183 with *T. gondii* driven cytokine expression. IL-6 production driven in this manner was not anti-
184 parasitic. Neutralisation of IL-6 in the presence or absence of cl-CD95L caused a decrease in
185 parasite numbers (Fig.2B). As previously demonstrated cl-CD95L caused an increase in
186 parasite number but this was reversed in the presence of anti-IL-6 (Fig.2B).

187 This led us to speculate that a second host factor, triggered by cl-CD95L, was responsible for
188 the effects on parasite load in BMDMs. To test this, we first assayed cl-CD95L treated and
189 infected BMDMs for arginase and found elevated levels following *T. gondii* infection but
190 treatment with cl-CD95L resulted in a further increase in these levels (Fig.2D). Indeed, the
191 effects of cl-CD95L induced increased arginase could be reversed with the application of the

192 inhibitor nor-NOHA. Simultaneous application of both cl-CD95L and nor-NOHA resulted in
193 significant decrease in parasite levels compared with cl-CD95L treatment only (Fig.2D); levels
194 of parasite obtained in cl-CD95L/nor-NOHA cultures were similar to those in non-treated
195 infected controls (Fig.2D). Interestingly, we found arginase-1 and IL-6 to be mechanistically
196 linked as nor-NOHA inhibition of arginase also caused a decrease in IL-6 levels during cl-
197 CD95L stimulation and infection (Supplementary Fig.1). STAT6 is a major transcriptional
198 regulatory of alternative activation of macrophages during helminth infection [11-13]. It has
199 been shown to drive the expression of arginase-1 during both cytokine and pathogen
200 stimulation. We employed chemical inhibition of STAT6 to determine if it was directing cl-
201 CD95L mediated arginase. During stimulation alone, cl-CD95L caused an increase in arginase-
202 1 activity (Fig.2F) but the application of a STAT6 inhibitor AS157499 caused a decrease in
203 these levels. Importantly following infection, we found that the synergistic increase in
204 arginase was also ablated (Fig.2F). Phenotypically inhibition of STAT6 gave rise to a lower
205 number of parasites but only after the application of cl-CD95L (Fig.2G; $P < 0.01$); suggesting
206 that cl-CD95L drives a STAT6 response, upregulating arginase, that mediates reduced
207 parasite killing. Our data above would indicate that IL-6 when induced by cl-CD95L is not
208 protective; to test if cl-CD95L:STAT6 signalling is involving in this we assayed supernatants
209 for IL-6 levels. We show that cl-CD95L drives a synergistic increase in IL-6 following *T. gondii*
210 infection ($P < 0.05$) and importantly STAT6 inhibition in this setting causes a complete
211 removal of IL-6 (Figure 2H).

212 3.3 cl-CD95L modifies the macrophage signalling landscape.

213 To address whether there was a pattern of cell signalling induced by cl-CD95L that could
214 underlie the effect on increased parasite replication, and associated immune responses in

215 BMDMs, we performed a Phospho-kinase profiler array on cl-CD95L stimulated BMDMs.
216 Exploring the cellular environment preceding infection was important and thus our
217 experimental design relied upon prior stimulation with cl-CD95L, as we had shown above
218 that this resulted in a cellular environment more permissive to parasite replication. 38 of 43
219 kinases were found to be expressed under both stimulated and unstimulated conditions.
220 Using a Log₂ fold change we identified 23 kinases upregulated in stimulated vs unstimulated
221 BMDMs (Fig.3A). These were subject to STRING (V11.0) analysis to identify potential
222 interactions using a database search. The top five Biological Processes and Reactomes are
223 depicted in Figure 3B. Not unexpectedly, 3 GO terms identified map to
224 phosphorylation/signal transduction and one to apoptotic processes. Cytokine signalling and
225 immune system responses were identified within the Reactome analysis.

226 A network was constructed from the log₂ fold upregulated proteins and three nodes are
227 apparent – one involving STATs, one centred on mTOR, and a third involving the Src family
228 (Yes, Fyn, Lck). Multiple members of these nodes, including Yes/Fyn/Lck, have significant
229 overlap with factors previously identified as being elicited by cl-CD95L [4, 7]. STAT2/3/5A
230 were identified in a node; STAT2 was previously shown to be negatively regulation immune
231 protection in *T. gondii* infection, as STAT2^{-/-} macrophages more effectively control their
232 parasite load [14]; while STAT3 mediates susceptibility to *T. gondii* [15, 16]; and STAT5 has
233 been implicated, albeit weakly, with increased parasite susceptibility [17].

234 The node centred on mTOR may indicate an MDSC-like response to cl-CD95L stimulation. A
235 role for MDSCs, and similar cells, have been subject to increasing scrutiny in the context of
236 parasite immunity [18]. Given the heterogeneous nature of their surface marker profile [18],
237 they may have potentially been incorporated into analysis of Gr1⁺ monocyte populations in

238 prior *T. gondii* studies [19-22] as many of these Gr1⁺ monocytes were also CD11b⁺. Indeed a
239 population corresponding to these cells was shown to exert both an anti-inflammatory
240 effect during infection and immune hyporesponsiveness during acute *T. gondii* infection
241 [22].

242

243

244

Journal Pre-proof

245 4. Discussion:

246 Increased levels of soluble CD95L have been found in both human toxoplasmosis and murine
247 macrophage infection. Given its potential effects outside of triggering cell death we
248 examined the effects of cl-CD95L on macrophage infection. Our findings lead us to conclude
249 that exposure of host cells to cl-CD95L leads to increased *T. gondii* replication and a parallel
250 rise in host cell destruction. Furthermore, this cell destruction is dependent on parasite
251 replication but not CD95L apoptotic effects as noted by our ATP findings. We determined
252 that IL-6 was also upregulated following cl-CD95L stimulated and *T. gondii* infection but this
253 was not protective as indicated by neutralising antibody. This finding is in line with previous
254 studies which also detail a role for IL-6 in promoting parasite intracellular replication [23]
255 conflicting with the protective role also assigned to IL-6 [24]. This contradictory nature of the
256 resulting macrophage population we obtained following cl-CD95L stimulation and *T. gondii*
257 infection reflects a previous finding that duality in the macrophage population can exist.
258 Arginase-1 has been widely reported to negatively impact upon immunity to intracellular
259 parasites [3] and this is known to arise from a key role in driving alternative activation of
260 macrophages[25]. Yap and colleagues have described a both classically and alternatively
261 activated macrophages existing within the same pool of cells following *T. gondii* infection
262 [26].

263 Combined, the data would suggest cl-CD95L drives STAT6 mediated expression of arginase-1
264 and IL-6; these factors may synergise with *T. gondii* infection to remove the protective
265 effects of IL-6 and increase the susceptibility of host cells in an arginase-dependent fashion.
266 This is consistent with prior reports of IL-6 acting to enhance alternative activation of
267 macrophages in a STAT3 dependent fashion [27]. Importantly, the autocrine/paracrine

268 induction of arginase-1 by IL-6, via STAT3, has also been shown during Mycobacteria
269 infection of macrophages [28]. Our Phospho-kinase array data revealed that STAT6 was
270 only one of multiple STAT members changed by cl-CD95L. Thus, here we show that the
271 actions of cl-CD95L in promoting parasite replication stem from STAT6 they may, at least
272 partially, from wider STAT signalling. Myeloid-derived suppressor cells have been linked to
273 both suppressing but also promoting inflammation in a variety of setting including systemic
274 lupus erythematosus (SLE) [29]; in this setting MDSCs expressing arginase-1 promoted Th17-
275 mediated kidney damage. This endstage pathology overlaps with our previous finding that
276 cl-CD95L drives selective recruitment of Th17 cells into tissues including in a murine model
277 of SLE [7]. A potential outcome of cl-CD95L stimulation of macrophages could be the
278 induction of an MDSC-like phenotype, independent of parasite infection. This is in part
279 supported by the finding that mTOR is upregulated as are a number of other kinases
280 associated with the MDSC phenotype. Our findings point to the need to closely examine the
281 role of cl-CD95L during *T. gondii* pathogenesis *in vivo* and to define the role it plays in
282 eliciting MDSCs. Specifically, does cl-CD95L elicit differentiation and trafficking of MDSCs and
283 what role do these cells play *in vivo*.

284

285 **Conflict of Interest:** RJF and PL are applicants on a patent surrounding the use of CD95
286 therapeutics.

287 **Acknowledgments:** We would like to thank Catherine Hartley for her technical assistance
288 and the staff at University of Liverpool Biomedical Services Unit. EAT was supported in part
289 through a Wellcome Trust ISSF award to RJF.

290

291 **References**

292

293

- 294 [1] Jensen KD, Wang Y, Wojno ED, Shastri AJ, Hu K, Cornel L, et al. Toxoplasma polymorphic effectors
295 determine macrophage polarization and intestinal inflammation. *Cell Host Microbe* 2011;9:472-83.
- 296 [2] Saeij JP, Collier S, Boyle JP, Jerome ME, White MW, Boothroyd JC. Toxoplasma co-opts host gene
297 expression by injection of a polymorphic kinase homologue. *Nature* 2007;445:324-7.
- 298 [3] El Kasmi KC, Qualls JE, Pesce JT, Smith AM, Thompson RW, Henao-Tamayo M, et al. Toll-like
299 receptor-induced arginase 1 in macrophages thwarts effective immunity against intracellular
300 pathogens. *Nat Immunol* 2008;9:1399-406.
- 301 [4] Tauzin S, Chaigne-Delalande B, Selva E, Khadra N, Daburon S, Contin-Bordes C, et al. The naturally
302 processed CD95L elicits a c-cyes/calcium/PI3K-driven cell migration pathway. *PLoS Biol*
303 2011;9:e1001090.
- 304 [5] Hu MS, Schwartzman JD, Yeaman GR, Collins J, Seguin R, Khan IA, et al. Fas-FasL interaction
305 involved in pathogenesis of ocular toxoplasmosis in mice. *Infect Immun* 1999;67:928-35.
- 306 [6] Vutova P, Wirth M, Hippe D, Gross U, Schulze-Osthoff K, Schmitz I, et al. Toxoplasma gondii
307 inhibits Fas/CD95-triggered cell death by inducing aberrant processing and degradation of caspase 8.
308 *Cell Microbiol* 2007;9:1556-70.
- 309 [7] Poissonnier A, Sanseau D, Le Gallo M, Malleter M, Levoine N, Viel R, et al. CD95-Mediated Calcium
310 Signaling Promotes T Helper 17 Trafficking to Inflamed Organs in Lupus-Prone Mice. *Immunity*
311 2016;45:209-23.
- 312 [8] El-Taweel HA, Abou-Holw SA, Ghoniem HM. Alteration in circulating soluble Fas level in
313 Toxoplasma seropositive pregnant women. *J Egypt Soc Parasitol* 2007;37:511-21.
- 314 [9] Guirelli PM, Angeloni MB, Barbosa BF, Gomes AO, Castro AS, Franco PS, et al. Trophoblast-
315 macrophage crosstalk on human extravillous under Toxoplasma gondii infection. *Placenta*
316 2015;36:1106-14.
- 317 [10] Edwards-Smallbone J, Pleass RJ, Khan NA, Flynn RJ. Acanthamoeba interactions with the blood-
318 brain barrier under dynamic fluid flow. *Exp Parasitol* 2012;132:367-72.
- 319 [11] Mishra BB, Gundra UM, Teale JM. STAT6(-)/(-) mice exhibit decreased cells with alternatively
320 activated macrophage phenotypes and enhanced disease severity in murine neurocysticercosis. *J*
321 *Neuroimmunol* 2011;232:26-34.
- 322 [12] Voehringer D, van Rooijen N, Locksley RM. Eosinophils develop in distinct stages and are
323 recruited to peripheral sites by alternatively activated macrophages. *J Leukoc Biol* 2007;81:1434-44.
- 324 [13] Zhao A, Urban JF, Jr., Anthony RM, Sun R, Stiltz J, van Rooijen N, et al. Th2 cytokine-induced
325 alterations in intestinal smooth muscle function depend on alternatively activated macrophages.
326 *Gastroenterology* 2008;135:217-25 e1.
- 327 [14] Ho J, Pelzel C, Begitt A, Mee M, Elsheikha HM, Scott DJ, et al. STAT2 Is a Pervasive Cytokine
328 Regulator due to Its Inhibition of STAT1 in Multiple Signaling Pathways. *PLoS Biol* 2016;14:e2000117.
- 329 [15] Butcher BA, Kim L, Panopoulos AD, Watowich SS, Murray PJ, Denkers EY. IL-10-independent
330 STAT3 activation by Toxoplasma gondii mediates suppression of IL-12 and TNF-alpha in host
331 macrophages. *J Immunol* 2005;174:3148-52.
- 332 [16] Portillo JC, Muniz-Feliciano L, Lopez Corcino Y, Lee SJ, Van Grol J, Parsons SJ, et al. Toxoplasma
333 gondii induces FAK-Src-STAT3 signaling during infection of host cells that prevents parasite targeting
334 by autophagy. *PLoS Pathog* 2017;13:e1006671.
- 335 [17] Jensen KD, Hu K, Whitmarsh RJ, Hassan MA, Julien L, Lu D, et al. Toxoplasma gondii rhopty 16
336 kinase promotes host resistance to oral infection and intestinal inflammation only in the context of
337 the dense granule protein GRA15. *Infect Immun* 2013;81:2156-67.

- 338 [18] Van Ginderachter JA, Beschin A, De Baetselier P, Raes G. Myeloid-derived suppressor cells in
339 parasitic infections. *Eur J Immunol* 2010;40:2976-85.
- 340 [19] Dunay IR, Damatta RA, Fux B, Presti R, Greco S, Colonna M, et al. Gr1(+) inflammatory
341 monocytes are required for mucosal resistance to the pathogen *Toxoplasma gondii*. *Immunity*
342 2008;29:306-17.
- 343 [20] Dunay IR, Sibley LD. Monocytes mediate mucosal immunity to *Toxoplasma gondii*. *Curr Opin*
344 *Immunol* 2010;22:461-6.
- 345 [21] Robben PM, LaRegina M, Kuziel WA, Sibley LD. Recruitment of Gr-1+ monocytes is essential for
346 control of acute toxoplasmosis. *J Exp Med* 2005;201:1761-9.
- 347 [22] Voisin MB, Buzoni-Gatel D, Bout D, Velge-Roussel F. Both expansion of regulatory GR1+ CD11b+
348 myeloid cells and anergy of T lymphocytes participate in hyporesponsiveness of the lung-associated
349 immune system during acute toxoplasmosis. *Infect Immun* 2004;72:5487-92.
- 350 [23] Beaman MH, Hunter CA, Remington JS. Enhancement of intracellular replication of *Toxoplasma*
351 *gondii* by IL-6. Interactions with IFN-gamma and TNF-alpha. *J Immunol* 1994;153:4583-7.
- 352 [24] Suzuki Y, Rani S, Liesenfeld O, Kojima T, Lim S, Nguyen TA, et al. Impaired resistance to the
353 development of toxoplasmic encephalitis in interleukin-6-deficient mice. *Infect Immun*
354 1997;65:2339-45.
- 355 [25] Gordon S. Alternative activation of macrophages. *Nat Rev Immunol* 2003;3:23-35.
- 356 [26] Patil V, Zhao Y, Shah S, Fox BA, Rommereim LM, Bzik DJ, et al. Co-existence of classical and
357 alternative activation programs in macrophages responding to *Toxoplasma gondii*. *Int J Parasitol*
358 2014;44:161-4.
- 359 [27] Fernando MR, Reyes JL, Iannuzzi J, Leung G, McKay DM. The pro-inflammatory cytokine,
360 interleukin-6, enhances the polarization of alternatively activated macrophages. *PLoS One*
361 2014;9:e94188.
- 362 [28] Qualls JE, Neale G, Smith AM, Koo MS, DeFreitas AA, Zhang H, et al. Arginine usage in
363 mycobacteria-infected macrophages depends on autocrine-paracrine cytokine signaling. *Sci Signal*
364 2010;3:ra62.
- 365 [29] Wu H, Zhen Y, Ma Z, Li H, Yu J, Xu ZG, et al. Arginase-1-dependent promotion of TH17
366 differentiation and disease progression by MDSCs in systemic lupus erythematosus. *Sci Transl Med*
367 2016;8:331ra40.

368

369

370 **Figure Legends:**

371 **Figure 1: Cleaved-CD95L alters *T. gondii* replication within host cells. (A)** VERO cells were
372 either stimulated with doses of cl-CD95L as indicated. After 24 hours the cells were then
373 infected with *T. gondii* at a MOI of 5 or left uninfected. After a further 48 hours post
374 infection the percentage of monolayer was estimated for each group by examination under
375 a light microscope. **(B)** VERO cells were either stimulated with 100ng/mL of cl-CD95L or left
376 unstimulated. After 24 hours the cells were then infected with *T. gondii* at a MOI of 5 or left
377 uninfected. After a further 48 hours post infection the parasite number was determined. **(C)**
378 Supernatants from the above experiment were tested for ATP using Cell Titer-Glo. **(D)** Bone
379 Marrow Derived Macrophages (BMDM) were either stimulated as in B). After 24 hours the
380 BMDM (10^5) were then infected and parasite counts as in B). **(E)** As in D) but in the presence
381 of Fas-Fc chimera (200ng/mL) or control antibody while undergoing cl-CD95L stimulation. All
382 culture conditions were in triplicate and mean \pm SD is shown with between 4-6 mice per
383 experiment. With experiments repeated independently 6 times in A) or 5 times in B)-E).
384 Data in (A), (C), and (E) were analysed by 2-way ANOVA and data in (B) and (D) by Unpaired
385 T-tests; *P<0.05, **P<0.01, and ***P<0.0001.

386

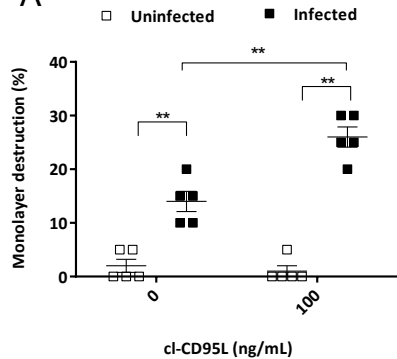
387 **Figure 2: cl-CD95L alters arginase-1 and IL-6 levels during *T. gondii* infection. A)** BMDM (10^5
388 per well) were stimulated using indicated doses of cl-CD95L. After 24 hours the BMDM were
389 then infected with *T. gondii* at a MOI of 5 or left uninfected. After a further 48 hours
390 supernatants were assayed for IL -6 by ELISA. **B) – H)** BMDMs were treated with cl-CD95L at
391 100ng/mL or 0ng/mL control prior to infection with *T. gondii* at MOI 5. **B)** The addition of
392 anti-IL-6 (120ng/mL) or control IgG was monitored for an effect on parasite counts as

393 performed in Figure 1. **C)** Arginase activity was measured 48hrs after infection cell lysates; **D)**
394 Inhibition of arginase was performed by addition of nor-NOHA (5mM) prior to measuring
395 parasite load; **E)** Matched cell lysates from B) were used to measure arginase activity after
396 anti-IL-6 treatment. STAT6 was inhibited (As1517499 – 0.2mg/mL) prior to infection and
397 during stimulation with cl-CD95L thereafter **F)** arginase activity was measured in cell lysates,
398 **G)** parasite numbers and **H)** IL-6 were measured in the supernatants. Treatments were
399 performed in triplicate and mean \pm SD is shown with 4-6 mice per experiment. Each
400 experiment was repeats 5 times independently. Data was analysed in GraphPad Prism by 2-
401 way ANOVA where *P<0.05, **P<0.01, ***P<0.001, ****P<0.0001.

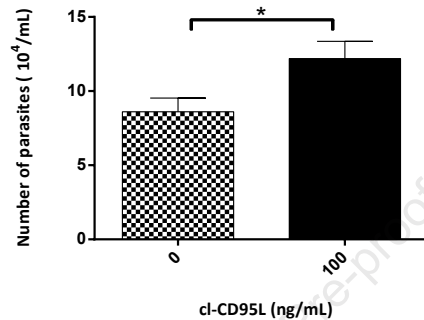
402 **Figure 3: cl-CD95L modifies the macrophage signalling landscape.** BMDM were treated with
403 100ng/mL of cl-CD95L for 24hrs prior to preparation for use in the Phospho-Kinase array
404 (R&D Systems). Pixel density captured in ImageJ was normalised to total protein levels. **A)**
405 Thereafter the Log₂ fold change in cl-CD95L stimulated vs unstimulated was calculated. The
406 blue dotted line indicates a Log₂ fold change while the red dotted line indicates a 2-Log₂ fold
407 change in expression levels. The 23 proteins with a Log₂ fold difference were then processed
408 in STRING V11.0 (string-db.org) program to identify potential interaction networks. B) The
409 top 5 biological processes and reactome pathways are identified presented. C) The potential
410 interaction network generated is presented, based upon known interactions taken from
411 InAct. The nature of the interaction is dictated as follows; lines with an arrowhead indicates
412 a positive interaction, lines with a rounded end indicate unknown interaction, lines with a
413 flat end indicate a negative end. Results shown are means from 2 independent biological
414 replicates for each treatment.

415

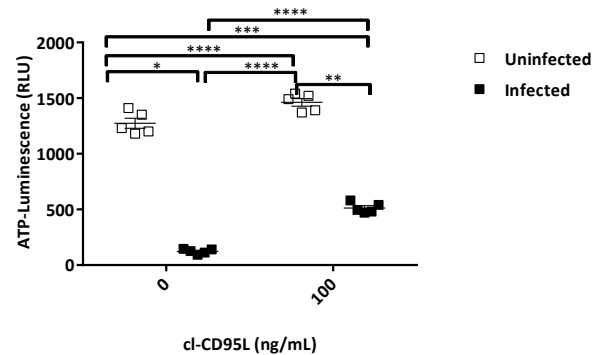
A



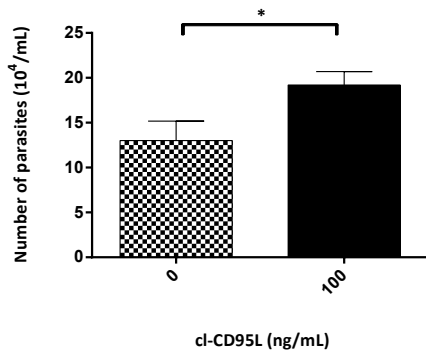
B



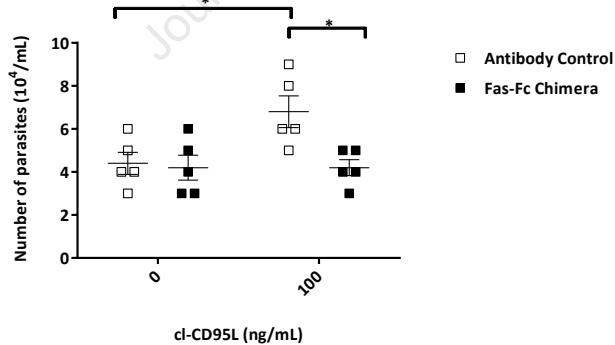
C



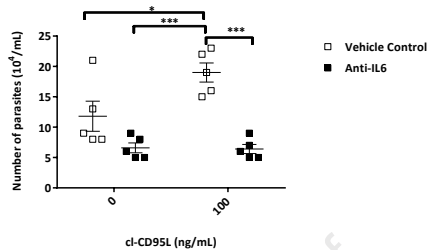
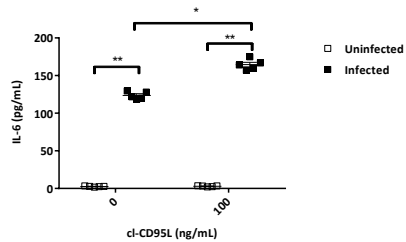
D



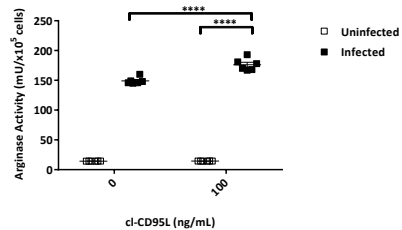
E



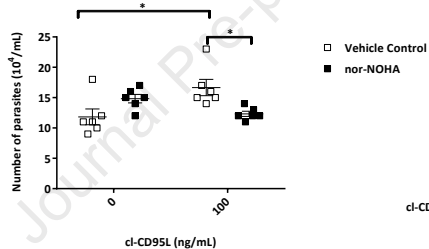
A



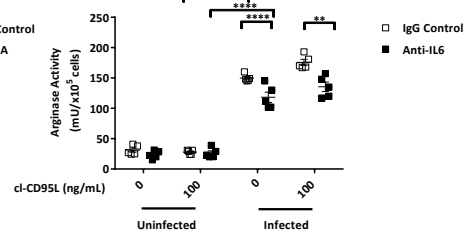
C



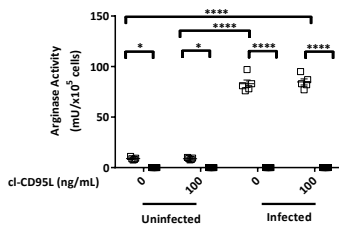
D



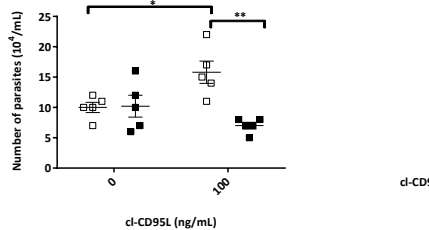
E



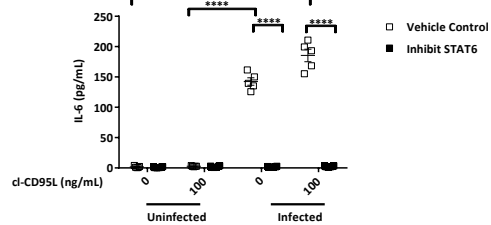
F



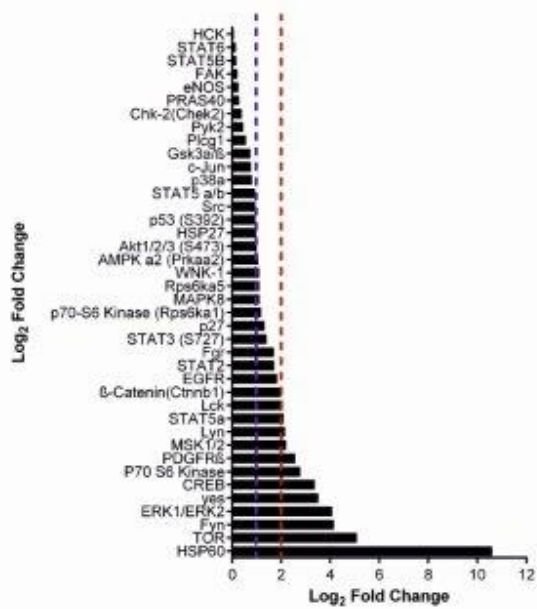
G



H



A



B

Biological Processes (GO)		
GO-term	Description	Count in network
GO:0007165	signal transduction	40 of 3594
GO:0006468	protein phosphorylation	28 of 793
GO:0042981	regulation of apoptotic process	32 of 1476
GO:0016310	phosphorylation	29 of 1034
GO:0071310	cellular response to organic substance	33 of 1858

Reactome Pathways		
Pathway	Description	Count in network
MMU-9006934	Signaling by Receptor Tyrosine Kinases	24 of 360
MMU-449147	Signaling by Interleukins	17 of 262
MMU-1280215	Cytokine Signaling in Immune system	18 of 357
MMU-168256	Immune System	26 of 1523
MMU-162582	Signal Transduction	30 of 2430

C

